Int. J. Solids Structures Vol. 15, pp. 261–267

0020-7683/79/0301-0261/$02.00/0

THE TIME-DEPENDENT DEFORMATION OF ICE DOMES

LESLIE E. HAJDO

Mechanical Engineering Department, University of Calgary, Calgary, Alberta, Canada T2N 1N4

(*Received* 6 *June* 1978; *in revised form* 25 *August* 1978; *received for publication* 31 *October* 1978)

Abstract—Thin shells of ice, constructed by spraying water onto an inflated membrane, could provide inexpensive winter shelters in the arctic. The major design consideration must be the creep behaviour of ice. In the present paper some time-dependent deformations of the proposed ice dome are obtained for the unloaded and snow-loaded situations.

1. INTRODUCTION

It has been proposed that ice domes would make suitable shelters in arctic regions[1]. They would be constructed by spraying water onto a cable-reinforced, inflated membrane. After the water solidifies, the membrane is to be removed for reuse, and the cables remain to reinforce the ice.

In the north, the use of ice domes can provide several advantages over more conventional construction. First, for the resource and exploration outfits, unheated or partially heated shelters, which provide temperatures of $-5°C$ with no wind, are adequate for equipment storage and repair shops. Second, the cost of transporting material to remote regions is very expensive. For the construction of ice domes, only relatively lightweight things such as the membrane, anchors, bolts and reinforcing cables need be flown in. Third, since the proposed domes are to be large enough to enclose several dormitory trailers and work areas, the inhabitants need not go outside between activities. Fourth, considerable savings in the consumption of fuel, which is very costly in remote regions, are likely. Vehicles can be sheltered and need not be kept running from autumn till spring. Also, less fuel would be required to maintain higher temperatures in the office and dormitory areas.

Small-scale testing of ice domes[1, 2], and studies of the time-dependent deformation of ice[3–7], show that ice shells require a more general analysis than that provided by linear elasticity. In its full generality, the deformation and stability analyses should consider viscoelastic behaviour, material and kinematic nonlinearities, the effects of the apertures, reinforcing, temperature, snow and wind loadings.

In this article, the dome is modelled as a linear Maxwell viscoelastic solid subject to self and snow loadings.

In Section 2 the theory and results for a dome deforming under its own weight are given. The effect of additional loading by snow is added in Section 3. The conclusions are drawn in Section 4.

2. UNLOADED ICE DOME

In the present work the ice dome is considered to be initially a section of a sphere without apertures. The envisaged ice domes are to be thin-shelled structures, 15 cm or so thick, with a projected surface radius r of up to 25 m (Fig. 1). Assuming that the ice takes on a polycrystalline state, it is assumed to be homogeneous and isotropic.

As discussed by Flügge[8], when a shell carries its load essentially by normal and shearing forces, then the moments may be neglected. The resulting simplified membrane theory allows the computation of forces and stresses based only upon the equations of statics. The primary loadings on ice domes are its own weight and the weight of the accumulated snow.

For a spherical dome under axisymmetric loading (Fig. 1), Flügge derives the stress resultants N_θ and N_ϕ to be

$$N_\theta = \frac{a}{\sin^2\theta}\int_0^\theta (p_r\cos\theta - p_\theta\sin\theta)\sin\theta\,\mathrm{d}\theta \tag{1}$$

$$N_\phi = ap_r - N_\theta \tag{2}$$

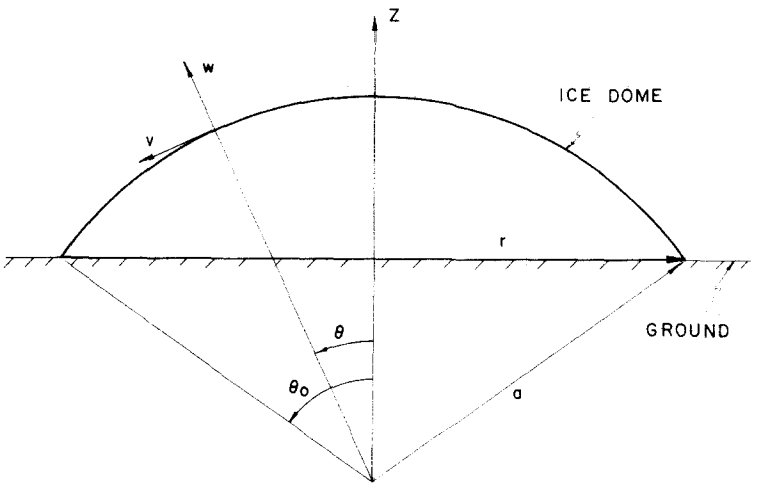

Fig. 1. Ice dome.

where a is the radius of the sphere, p is the shell's weight per unit area of the middle surface, and

$$p_\theta = p \sin\theta; \quad p_r = -p \cos\theta. \tag{3}$$

For a uniform shell, p is a constant, and one obtains

$$N_\theta = \frac{-pa}{1+\cos\theta} \tag{4}$$

$$N_\phi = pa\left[\frac{1}{1+\cos\theta} - \cos\theta\right]. \tag{5}$$

For a shell thickness τ, $p = \rho g\tau$ where ρ is the mass density and g is the gravitational constant. If the stresses are approximated by dividing the stress resultants by τ, then these become

$$\sigma_\theta = -\rho ga\left[\frac{1}{1+\cos\theta}\right] \tag{6}$$

$$\sigma_\phi = \rho ga\left[\frac{1}{1+\cos\theta} - \cos\theta\right]. \tag{7}$$

Note that for a self-loaded membrane the stresses are independent of thickness. For a surface radius $r = a \sin\theta_0 = 25$ m, $\theta_0 = 45°$, $\rho = 917$ kg/m^3 and $g = 9.81$ m/sec^2, the stresses are illustrated in Fig. 2.

The difficulty in treating ice in general is that it is a nonlinear viscoelastic solid. While it seems certain[4, 5] that this nonlinearity is high for high stresses, there appears to be little agreement for low stresses[5–7]. Variations in sample preparation and difficulties with keeping experimental conditions constant are most likely the causes of the disagreements. The data given by Stanley[3], Bromer and Kingery[7], and some of the results of Jellinek and Brill[4] indicate that if one is not particularly interested in the strain shortly after loading, then the deformation of ice can be separated into an elastic part and a subsequent viscous fluid flow. Such behaviour is typical of Maxwell solids. For instance, from [7], it may be shown that the strain rate $\dot{\epsilon}$ is

$$\dot{\epsilon} = \gamma(\sigma)\sigma \tag{8}$$

where the material modulus γ(Pa^{-1} s^{-1}) at -13.0°C is

$$\gamma(\sigma) = 2.9 \times 10^{-5}\sigma^{0.0809} \tag{9}$$

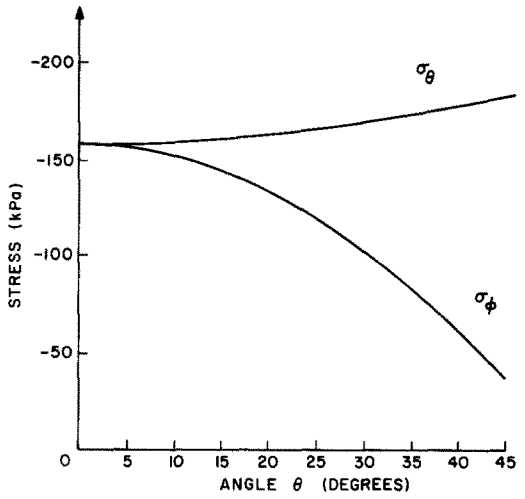

Fig. 2. Stresses in an unloaded spherical dome as a function of angle.

with σ in Pascals. Although this still represents a nonlinear rate of strain, γ's dependence on σ is very small and will be neglected. It is not difficult to show from [9] that for viscous flow

$$\dot{\epsilon}_\theta = \gamma\sigma_\theta - \pi\sigma_\phi \tag{10}$$

$$\dot{\epsilon}_\phi = \gamma\sigma_\phi - \pi\sigma_\theta \tag{11}$$

where π is a material modulus. In the present article it is assumed that γ is a constant, given by the worst case, i.e. the highest stress anywhere in the shell. Since no data appear to be available for π, which plays the same role here as does ν/E, Poisson's ratio divided by Young's modulus, in elasticity theory, it is assumed that

$$\pi = \gamma\nu. \tag{12}$$

Integrating (10) and (11) with respect to time gives

$$\epsilon_\theta = (\gamma\sigma_\theta - \pi\sigma_\phi)t + \epsilon_1 \tag{13}$$

$$\epsilon_\phi = (\gamma\sigma_\phi - \pi\sigma_\theta)t + \epsilon_2 \tag{14}$$

where t is time and ϵ_1 and ϵ_2 are the elastic strains. From geometric consideration Flügge obtains [8]

$$\epsilon_\theta = \frac{1}{a}\left[\frac{\partial v}{\partial\theta} + w\right] \tag{15}$$

$$\epsilon_\phi = \frac{1}{a}[v\cot\theta + w] \tag{16}$$

where v and w are the tangential and perpendicular displacements (Fig. 1). Solving the differential equations which result from the combination of (13)–(16), following [8] one obtains

$$v = \sin\theta\left\{\int_0^\theta [(\gamma+\pi)(\sigma_\theta - \sigma_\phi)t + \epsilon_1 - \epsilon_2]\frac{a}{\sin\theta}\,d\theta + C\right\}. \tag{17}$$

From Hooke's law

$$E\epsilon_1 = \sigma_\theta - \nu\sigma_\phi \tag{18}$$

$$E\epsilon_2 = \sigma_\phi - \nu\sigma_\theta \tag{19}$$

eqn (17) becomes

$$v = \sin\theta\left\{\int_0^\theta (mt+n)\left(\cos\theta - \frac{2}{1+\cos\theta}\right)\frac{d\theta}{\sin\theta} + C\right\} \tag{20}$$

where

$$m \equiv \frac{pa^2}{\tau}(\gamma+\pi) \qquad n \equiv \frac{pa^2}{\tau E}(1+\nu). \tag{21}$$

Integration of (20) gives

$$v = C\sin\theta + (mt+n)\sin\theta\left[\ln\left(\frac{\sin\theta}{\tan\theta/2}\right) - \frac{1}{1+\cos\theta}\right]_{\theta_0}^{\theta}. \tag{22}$$

From (6), (7), (14), (16) and (19) one gets

$$w = \frac{pa^2}{E\tau}\left[\frac{tE(\gamma+\pi)+1+\nu}{1+\cos\theta} - (t\gamma E+1)\cos\theta\right] - v\cot\theta. \tag{23}$$

In membrane theory only one displacement boundary condition may be satisfied. Here, it is required that there be no vertical motion at $\theta = \theta_0$. At the boundary

$$v = C\sin\theta_0 \tag{24}$$

$$w = \frac{pa^2}{\tau E}\left[\frac{tE(\gamma+\pi)+1+\nu}{1+\cos\theta_0} - (t\gamma E+1)\cos\theta_0\right] - C\cos\theta_0. \tag{25}$$

Demanding that $w\cos\theta_0 = v\sin\theta_0$ produces

$$C = \left[\frac{mt+n}{1+\cos\theta_0} - \frac{pa^2}{\tau E}(t\gamma E+1)\cos\theta_0\right]\cos\theta_0. \tag{26}$$

Equations (22), (23) and (26) were evaluated numerically for a number of cases. Equations (22) and (23) are well-behaved at $\theta = 0$. However, for θ at, or near 0, the computer cannot handle the 0/0 and $0\cdot\infty$ that occur in (22) and (23). It is straightforward to obtain analytic expressions for (22) and (23) for θ approaching zero. These were used wherever appropriate in the numerical computation.

For the value of ρ, τ and g given earlier, p is 1349 N/m^2. From [3] and [10], E and ν were taken to be 7.0 GPa and 0.4, respectively. Using the largest stress in Fig. 2, $|-186|$ kPa, γ and π were computed using (9) and (12) to be 0.77×10^{-14} Pa^{-1} s^{-1} and 0.31×10^{-14} Pa^{-1} s^{-1}. Figure 3 presents the deformations at $t = 10^7$ s (115.6 days). The elastic components of the displacements are of the order of millimetres.

3. DOME LOADED BY SNOW

Given the vagaries of the settlement of snow under various temperature and wind conditions, it is difficult to determine accurately the effect of a snow load on the dome. It appears reasonable to assume that snow accumulation on a surface approaches zero as the angle of repose of that surface tends to the vertical. The weight per unit surface area of the dome and snow is taken to be

$$p_\theta = (p + s\cos\theta)\sin\theta \tag{27}$$

$$p_r = -(p + s\cos\theta)\cos\theta \tag{28}$$

where s is the weight of snow per unit area accumulating on a horizontal surface. Substituting

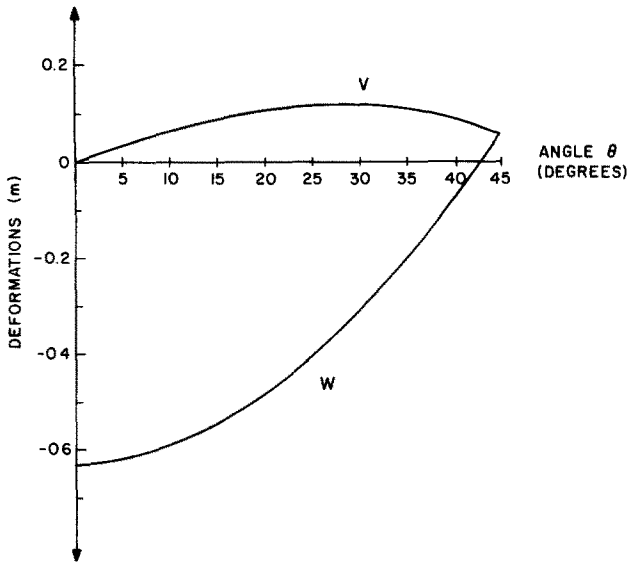

Fig. 3. Deformations after 10^7 sec. in an unloaded, initially spherical dome as a function of angle.

(27) and (28) into (1) produces

$$N_\theta = -\frac{pa}{1+\cos\theta} - \frac{s}{2}. \tag{29}$$

From (4) one also gets

$$N_\phi = pa\left[\frac{1}{1+\cos\theta} - \cos\theta\right] - \frac{as}{2}\cos 2\theta. \tag{30}$$

Following the same procedure as in Section 2, the following integral form for v is obtained.

$$v = C\sin\theta + (mt+n)\sin\theta\int_0^\theta \left(\cos\theta - \frac{2}{1+\cos\theta}\right)\frac{d\theta}{\sin\theta}$$
$$-\frac{a^2 s}{\tau}\sin\theta\int_0^\theta\left[(\gamma+\pi)t + \frac{(1+\nu)}{E}\right]\sin\theta\,d\theta. \tag{31}$$

The constants are as defined earlier, except for C which must be reevaluated. Integration of (31) produces

$$v = \sin\theta\left\{C + (mt+n)\left[\ln\left(\frac{\sin\theta}{\tan\theta/2}\right) - \frac{1}{1+\cos\theta} + \frac{s}{p}\cos\theta\right]_{\theta_0}^{\theta}\right\}. \tag{32}$$

And, after some algebra, w is obtained as

$$w = \frac{pa^2}{\tau E}\left[\frac{Et(\gamma+\pi)+1+\nu}{1+\cos\theta} - (t\gamma E+1)\cos\theta\right] - v\cot\theta + \frac{sa^2}{2\tau E}[Et(\pi - \gamma\cos 2\theta) + \nu - \cos 2\theta]. \tag{33}$$

Demanding that there be no vertical motion at $\theta = \theta_0$ determines the constant C. Hence, applying $w\cos\theta_0 = v\sin\theta_0$ gives

$$C = \cos\theta_0\left[\frac{mt+n}{1+\cos\theta_0} - \frac{pa^2}{\tau E}(t\gamma E+1)\cos\theta_0\right] + \frac{sa^2}{2\tau E}\cos\theta_0[Et(\pi - \gamma\cos 2\theta_0) + \nu - \cos 2\theta_0]. \tag{34}$$

The previously utilized computer programme was modified according to the present formulae. The stresses obtained are shown in Fig. 4. For illustrative purposes, it was assumed that $s = 1500\,\mathrm{N/m^2}$, which is slightly more than the weight of a 15 cm thick shell. The other parameters were unchanged. From the value of the largest stress, $|-363|$ kPa, γ and π were computed to be 0.817×10^{-14} $\mathrm{Pa^{-1}\ s^{-1}}$ and 0.327×10^{-14} $\mathrm{Pa^{-1}\ s^{-1}}$, respectively. Then, the deformations after 10^7 s (115.6 days) were calculated, giving the values shown in Fig. 5. Again, the elastic components of the displacements are only of the order of millimetres.

4. CONCLUSIONS

The domes that have been discussed in this article have a central height of 7.3 m. The sags at the centre after 10^7 s were 0.63 and 1.54 m, respectively, for the unloaded and snow-loaded situations. These values represent 8.6 and 21.0% reductions in the ceiling heights. For the unloaded dome, the thickness does not affect the stresses or deformations. Of course, for domes subject to external loads such as snow or wind, greater thicknesses provide better creep resistance. This may be seen by observing that the second terms in (29) and (30) become less significant as τ and hence p increase.

The easiest method of improving the creep characteristics of ice domes is to use smaller dimensions. An unloaded dome with $r = 15$ m and $\theta_0 = 45°$ develops a maximum stress of -111 kPa. The sag at the centre is 0.217 m with an initial ceiling height of 4.39 m. This is a relatively smaller deformation (5%), than that obtained for the larger dome.

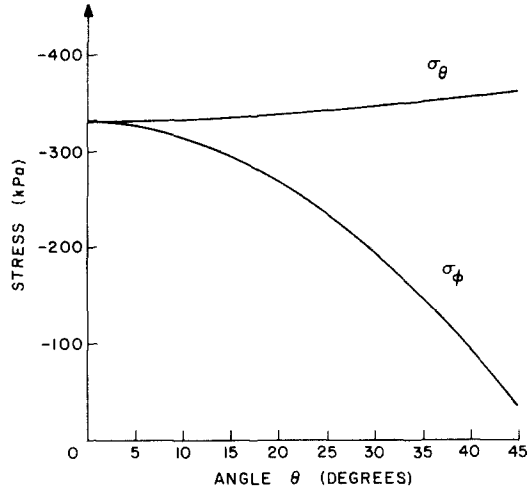

Fig. 4. Stresses in a snow-loaded dome as a function of angle.

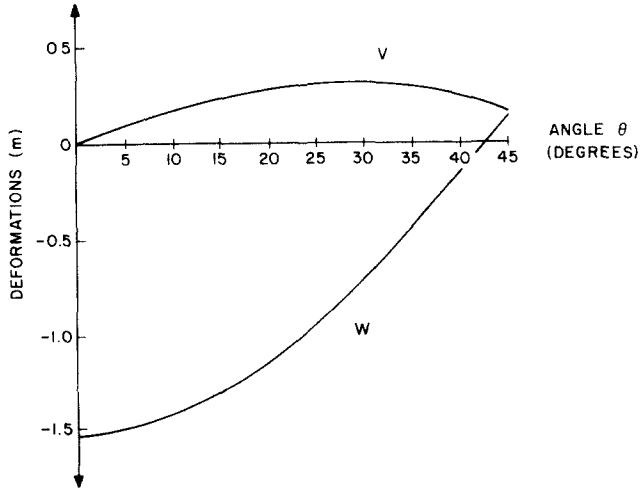

Fig. 5. Deformations after 10^7 sec. in a snow-loaded, initially spherical dome as a function of angle.

The results indicate that although large-scale ice domes appear to be feasible for winter shelter, the creep deformations are by no means insignificant. The creep is neither so great as to cause insurmountable difficulties, nor so small as to be ignorable. The approximations made in this paper are divided between conservative and optimistic. The benefits of cable-reinforcing were neglected and the material modulus γ was assumed to be at the upper bound of its range over the shell. On the other hand, the destabilizing effect of wind, which is very significant in the north, was omitted. Possible stress concentrations near apertures were neglected. There is evidence [3], however, that cable-reinforcing is most effective in these locations, so this omission may not be too serious. Perhaps most importantly, temperature variations were neglected. At higher temperatures, $-5°C$ or greater, the creep rates of ice increase considerably [3–5].

It is planned in future work to relax some of the more severe assumptions of the present theory.

Acknowledgements—The author gratefully acknowledges Dr. P. G. Glockner's suggestion of this problem and several discussions with him and Dr. D. J. Malcolm. This work was supported by Grant No. 69-1156 from the University of Calgary.

REFERENCES

1. R. G. Stanley and P. G. Glockner, The use of reinforced ice in constructing temporary enclosures. *Marine Sci. Commun.* **1**(6), 447–462 (1975).
2. R. G. Stanley and P. G. Glockner, Reinforced Ice: Its Properties and Use in Constructing Temporary Enclosures. *Proc. 3rd Int. Conf. Port and Ocean Engineering under Arctic Conditions*, University of Alaska, Fairbanks (11–15 August 1975).
3. R. G. Stanley, Reinforced Ice Domes. Master's Thesis, Department of Civil Engineering, The University of Calgary, Calgary, Alberta (1975).
4. H. H. G. Jellinek and R. Brill, Viscoelastic properties of ice. *J. Appl. Phys.* **27**(10), 1198–1209 (1956).
5. J. W. Glen, The creep of polycrystalline ice. *Proc. R. Soc.* **A228**, 519–538 (1955).
6. M. Mellor and R. Testa, Creep of ice under low stress. *J. Glaciology* **8**(52), 147–152 (1969).
7. D. J. Bromer and W. D. Kingery, Flow of polycrystalline ice at low stresses and small strains. *J. Appl. Phys.* **39**(3), 1688–1691 (1968).
8. W. Flügge, *Stresses in Shells*, 2nd Edn. Springer-Verlag, New York (1973).
9. A. C. Eringen, *Mechanics of Continua*, Chap. 9. Wiley, New York (1967).
10. L. W. Gold, Some Bulk Properties of Ice. *Tech. Paper No.* 256, D. B. R., National Research Council of Canada.